



## Preliminary results of core-edge simulations of *H*-mode tokamak plasmas using

### BALDUR and TASK codes

Yutthapong Pianroj<sup>1</sup>, Atsushi Fukuyama<sup>2</sup>, Thawatchai Onjun<sup>\*1</sup>, Sujin Suwanna<sup>1</sup>,  
Nopporn Poolyarat<sup>3</sup> and Roppon Picha<sup>4</sup>

<sup>1</sup> School of Manufacturing Systems and Mechanical Engineering, Sirindhorn International Institute of Technology, Thammasat University, Pathumthani, Thailand, 12120

<sup>2</sup> Department of Nuclear Engineering, Faculty of Engineering, Kyoto University, Kyoto, Japan

<sup>3</sup> Department of Physics, Faculty of Science, Thammasat University, Bangkok, Thailand

<sup>4</sup> Thailand Institute of Nuclear Technology, Bangkok, Thailand

\*Corresponding Author: thawatchai@siit.tu.ac.th, Tel. 66(2)564-3221-9, Fax. 66(2)986-9112-3

#### **Abstract**

A theory-based model for predicting the pedestal formation of temperature and density in *H*-mode plasma is used together with a core transport model in the 1.5D BALDUR and TASK integrated predictive modeling codes to self-consistently simulate *H*-mode plasmas. In the core plasma, an anomalous transport is computed using a semi-empirical Mixed Bohm/gyro-Bohm (Mixed B/gB), while a neoclassical transport is computed using the NCLASS model. For the pedestal, the electron and ion thermal, particle and impurity transports are suppressed individually due to the influence of  $\omega_{E \times B}$  flow shear. Because of the reduction of transport, the pedestal can be formed. The core-edge model is used to simulate the time evolution of plasma current, temperature, and density profiles for DIII-D tokamaks. A statistical analysis (percent of root mean square error, RMSE) is used to quantify the agreement with the experimental DIII-D data. The simulation results show a good agreement, with RMSE of less than 20%.

**Keywords:** Plasma, Nuclear fusion, Tokamak, Plasma, Transport barriers

## 1. Introduction

Nuclear fusion is the reaction that fuses light nuclei such as a deuteron (D) and a triton (T) to create heavier nuclei such as a helium nucleus. One of the techniques used to confine hot plasmas in order to sustain fusion reactions is the magnetic confinement. To produce a significant fusion reaction in magnetically confined plasma, a fusion reactor requires conditions such as a temperature in the order of a hundred million degrees Kelvin, the density in the order of  $10^{20}$  particles/m<sup>3</sup>, and the confinement time in the order of a few seconds. A magnetic confinement fusion uses a strong magnetic field to keep the hot plasma away from the surface of the chamber walls. One type of the magnetic confinement device is named "tokamak", which has a toroidally shaped chamber and relies on two components of the magnetic field to confine the plasma [1]. A major advance in magnetic confinement fusion happened with the discovery of the new operation regime, called the "High confinement mode" (*H*-mode) [2]. The *H*-mode operation results in a significant increase in the plasma temperature and confinement time compare with the "Low confinement mode" (*L*-mode). The radial pressure profiles for a typical *L*-mode and *H*-mode discharge are depicted in Fig.1. It can be seen that there is a significant increase in the plasma core temperature profile from the *L*-mode to the *H*-mode. The large increasing is the result of a transport barrier that forms at the edge of the *H*-mode plasma. This edge transport barrier (ETB) is usually referred to the "pedestal". Typically, the energy content in an *H*-mode discharge is approximately twice the

energy contained in an *L*-mode discharge, for the plasma heated with the same input power.

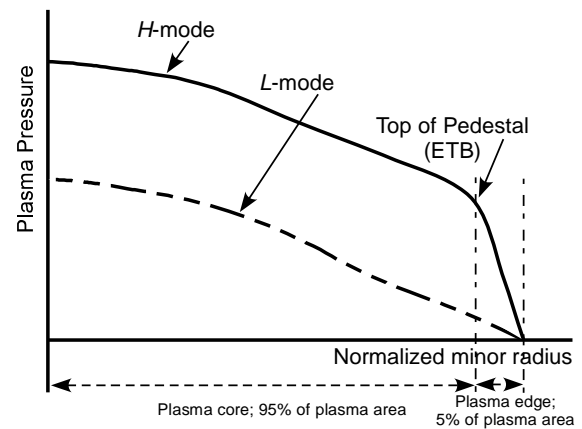


Fig. 1 Pressure profiles are plotted as function normalized minor radius for *L*-mode and *H*-mode plasma.

To develop a better understanding of the physical processes and the interrelationships between those physical processes that occurs in tokamak plasma experiments, advanced computer codes are developed to improved understand of plasma behaviors. The integrated predictive modeling codes, such as the BALDUR code [3], the TASK/TR code [4], the JETTO code [5], the ASTRA code [6] and the CRONOS code [7], play an important role in carrying out simulations in order to predict the time evolution of plasma current, temperature, and density profiles. However, many of the simulations carried out with these integrated predictive modeling codes make use of boundary conditions taken from experimental data. In simulating *H*-mode discharge, the evolution of the core plasma was carried out using boundary conditions taken from experimental data at the top of the pedestal [8-13], because the area from the top of the pedestal to the center of plasma is approximately 95% of the total area,



as shown in Fig.1. The edge occupies only the remaining 5% of the area; this calls for the plasma edge to be ignored. Several years after discovery of the  $H$ -mode scenario, however, the researchers found the different physical phenomena at the plasma edge area such as the  $L$ - $H$  transition, the formation of pedestal and edge localized modes (ELMs) that have influences to the plasma core area. These phenomena suggest that the integrated predictive modeling code must be extended to include the entire plasma cross section area, because the reliable methodology to predict the plasma properties is needed in order to advance the predictive capability. This capability is essential in designing future experiments in existing tokamaks.

The requirement for formation of the pedestal is the reduction of fluctuation driven transport. This can be achieved by stabilization or decorrelation of microturbulence in the plasma. The stabilization mechanisms, which can suppress turbulent modes, have to account for the different dynamical behaviors of the various species in the plasma. The first candidate for edge turbulence stabilization is the  $E \times B$  flow shear. The  $E \times B$  flow shear can suppress turbulence by linear stabilization of turbulent modes, and in particular by non-linear decorrelation of turbulence vortices [14-16], thereby reducing transport by acting on both the amplitude of the fluctuations and the phase between them [17]. The second candidate is additional magnetic shear stabilization ( $s$ ), which is reduced only in the region where the shear  $s$  exceeds the threshold and is unaffected

elsewhere; more details will be explained in section 2.3.2.

This paper is organized as follows: the details of edge model with suppression factor that has been developed will be described in next section, then brief information of the Mixed Bohm/gyro-Bohm (Mixed B/gB) anomalous core transport, and the integrated predictive modeling code BALDUR and TASK/TR are described in Section 3 and 4, respectively. In Section 5, the simulation results for standard  $H$ -mode will be validated by the statistical comparisons with the experimental data from DIII-D tokamak. The final section is the conclusion.

## 2. Modeling of Edge Plasma

The major purpose of modeling the edge transport is to understand and predict the formation of the pedestal structure such as the variation of the pedestal width and height for the plasma density and temperature. Therefore, the modeling of pedestal structure inevitably requires the full integration with the core and scrape-off layer (SOL)/divertor plasmas. Thus, one of the difficulties in modeling the pedestal structure is that there exist various physical mechanisms with very different time scales. The pedestal structure evolves on a transport time scale, but during this evolution, magnetohydrodynamic (MHD) phenomena with very short time scales occur, as from type-I edge localized modes (ELMs) [18]. The occurrence of an MHD event (ELM) burst produces a significant pulsed flow of particles and energy onto the divertor target, diminishing the edge pressure gradients in the process. Thus, the modeling of the transport barrier width is not yet well developed. An appropriate transport suppression factor ( $f_s$ ) due



to  $\omega_{E \times B}$  flow shearing rate together with the reduction of turbulence growth rate [19-21] and the magnetic shear [22, 23] can be shown in Eq.(1). Moreover, we assume all the simulations evolved the temperature pedestal width and height during the ELM-free phase.

$$f_{s_x} = \frac{1}{C_x \left( \frac{\omega_{E \times B}}{YITG} \right)^2} \times \frac{1}{\max(1, (s-0.5)^2)} \quad (1)$$

where,  $C_x$  is the calibration parameters for each species,  $s$  is the magnetic shear. The suppression of ion thermal diffusivity ( $\chi_{i_s}$ ), suppression of electron thermal diffusivity ( $\chi_{e_s}$ ), suppression of hydrogenic particle diffusivity ( $D_{H_s}$ ) and suppression of impurity particle diffusivity ( $D_{z_s}$ ) are given by Eq.(2-5).

$$\chi_{i_s} = \chi_i \times f_{s_{ion}} \quad (2)$$

$$\chi_{e_s} = \chi_e \times f_{s_{electron}} \quad (3)$$

$$D_{H_s} = D_H \times f_{s_{Hydrogenic}} \quad (4)$$

$$D_{z_s} = D_z \times f_{s_{impurity}} \quad (5)$$

### 3 Modeling for Core

The Mixed B/gB core transport model [24] is an empirical transport model. It was originally a local transport model with Bohm scaling. A transport model is said to be "local" when the transport fluxes (such as heat and particle fluxes) depend entirely on local plasma properties (such as temperatures, densities, and their gradients). A transport model is said to have "Bohm" scaling when the transport diffusivities are proportional to the gyro-radius times thermal velocity over a plasma linear dimension such as major radius. Transport diffusivities in models with Bohm scaling are also functions of the profile shapes (characterized by normalized gradients) and other plasma

parameters such as magnetic  $q$ , which are all assumed to be held fixed in systematic scans in which only the gyro-radius is changed relative to plasma dimensions. The original JET model was subsequently extended to describe ion transport, and a gyro-Bohm term was added in order for simulations to be able to match data from smaller tokamaks as well as data from larger machines. A transport model is said to have "gyro-Bohm" scaling when the transport diffusivities are proportional to the square of the gyroradius times thermal velocity over the square of the plasma linear dimension. The Bohm contribution to the JET model usually dominates over most of the radial extent of the plasma. The gyro-Bohm contribution usually makes its largest contribution in the deep core of the plasma and plays a significant role only in smaller tokamaks with relatively low power and low magnetic field. The Mixed B/gB transport model can be expressed as follows[25]:

$$\chi_e = 1.0\chi_{gB} + 2.0\chi_B \quad (6)$$

$$\chi_i = 0.5\chi_{gB} + 4.0\chi_B + \chi_{neo} \quad (7)$$

$$D_H = [0.3 + 0.7\rho] \frac{\chi_e \chi_i}{\chi_e + \chi_i} \quad (8)$$

$$D_z = D_H \quad (9)$$

where,

$$\chi_{gB} = 5 \times 10^{-6} \sqrt{T_e} \left| \frac{\nabla T_e}{B_\phi^2} \right| \quad (10)$$

$$\chi_B = 4 \times 10^{-5} R \left| \frac{\nabla(n_e T_e)}{n_e B_\phi} \right| q^2 \left( \frac{T_{e,0.8} - T_{e,1.0}}{T_{e,1.0}} \right) \times \Theta \left( -0.14 + s - \frac{1.47 \omega_{E \times B}}{YITG} \right) \quad (11)$$

where,  $\chi_e$  is the electron diffusivity,  $\chi_i$  is the ion diffusivity,  $D_H$  is the particle diffusivity,  $D_z$  is the impurity diffusivity,  $\chi_{gB}$  is the gyro-Bohm contribution,  $\chi_B$  is Bohm contribution,  $\rho$  is



normalized minor radius,  $T_e$  is the electron temperature in keV,  $B_\phi$  is the toroidal magnetic field,  $R$  is the major radius,  $n_e$  is the local electron density,  $q$  is the safety factor,  $s$  is the magnetic shear  $\omega_{E \times B}$  is the flow shearing rate and the  $\gamma_{ITG}$  is the ion temperature gradient (ITG) growth rate, estimated as  $v_{ti}/qR$  [26], in which  $v_{ti}$  is the ion thermal velocity.

#### 4. Integrated Predictive Modeling Codes

The transport models, which are used in both integrated predictive modeling codes; BALDUR and TASK/TR, take into account the two main regions of the plasma. The first transport model named the Mixed Bohm/gyro-Bohm (Mixed B/gB) describes the transport phenomena in the plasma core region. The other model describes the plasma edge region. The details of both transport models are described in the previous section.

##### 4.1 BALDUR

BALDUR is used to compute the time evolution of plasma profiles including electron and ion temperatures, deuterium and tritium densities, helium and impurity densities, magnetic  $q$ , neutrals, and fast ions. These time-evolving profiles are computed by combining the effects of many physical processes self-consistently, including the effects of transport, plasma heating, particle influx, boundary conditions, the plasma equilibrium shape, and sawtooth oscillations. Fusion heating and helium ash accumulation are also computed self-consistently. The BALDUR simulations have been intensively compared against various plasma experiments, which yield an overall agreement of 10% RMS deviation [12, 13]. In BALDUR code, fusion heating power is

determined using the nuclear reaction rates and a Fokker Planck package to compute the slowing down spectrum of fast alpha particles on each flux surface in the plasma. The fusion heating component of the BALDUR code also computes the rate of production of thermal helium ions and the rate of depletion of deuterium and tritium ions within the plasma core. The brief details of these transport models are described below.

##### 4.2 TASK/TR

TASK/TR transport code is based on solving a set of diffusive transport equations. The code [27] calculates a temporal evolution of the density and temperature for every species of particles in the core plasma: electrons, deuteriums, tritiums, thermalized  $\alpha$  particles, neutrals, multiple impurities and the other particles. The TASK/TR transport code solves one-dimension diffusive equation for densities, temperature and a poloidal magnetic flux with respect to the normalized minor radius  $\rho$ . The effect of  $E \times B$  shear stabilization is considered to be important to allow plasma to form a transport barrier. Applying this effect appropriately for simulation, the TASK/TR calculates the radial electric field, which is derived by the radial ion force balance. It should be noted that the toroidal velocity used from the experimental data and every discharge in the profile database does not always contain the toroidal velocity data. Therefore we multiply the toroidal angular speed by the surface averaged geometrical major radius, both of which are usually included in the database. The poloidal velocity is computed using the NCLASS module. Moreover, the TASK/TR includes various

neoclassical transport models to evaluate the transport coefficients, the bootstrap current, the neoclassical resistivity and the poloidal flow velocity and viscosity.

## 5. Results and Discussions

### 5.1 Simulated Plasma Profiles

All the experimental data from 10 DIII-D *H*-mode discharges considered in this paper are taken from [13, 28]. These experimental data are used as the initial and boundary conditions for the core simulations and core-edge simulations. However, the simulation results which are carried out by the core model are calculated at the top pedestal that depends on the boundary conditions of each discharge.

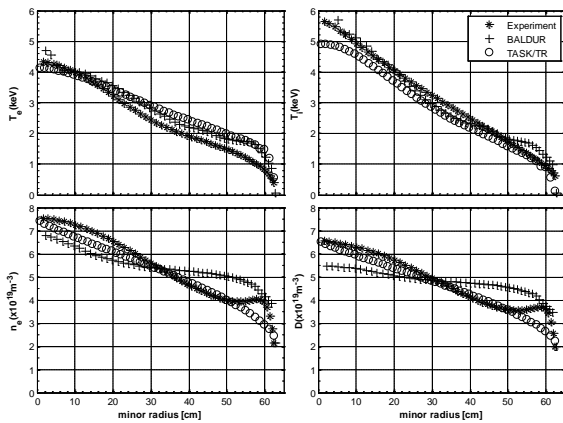


Fig. 2 The profile of electron temperature, ion temperature electron density and deuterium density as a function of minor radius. The simulation results are carried out by BALDUR

and TASK/TR with core-edge transport model compared to the DIII-D experimental data discharge 82205 at time 3.025 second.

The simulation results which carried out by core-edge model are calculated at the plasma edge with the same temperature 0.01 keV and compared with the DIII-D experiment data discharge 82205 are depicted in Fig.2.

### 5.2 Statistical analysis

To quantify the comparison between simulations and experiments, the percentage of root-mean-square error (%RMSE) deviation is computed based on the difference between simulation results and experimental data. In this paper, the %RMSE is defined as Eq. (12).

$$\%RMSE = \sqrt{\frac{1}{N} \sum_{i=1}^N \left( \frac{X_{exp_i} - X_{sim_i}}{X_{exp_0}} \right)^2} \times 100 \quad (12)$$

where,  $X_{exp_i}$  is the  $i$ th data point of the experimental profile,  $X_{sim_i}$  is the corresponding data point of the simulation profile and  $X_{exp_0}$  is the maximum data point of the experimental profile of  $X$  as a function of radius, which has  $N$  points in total.

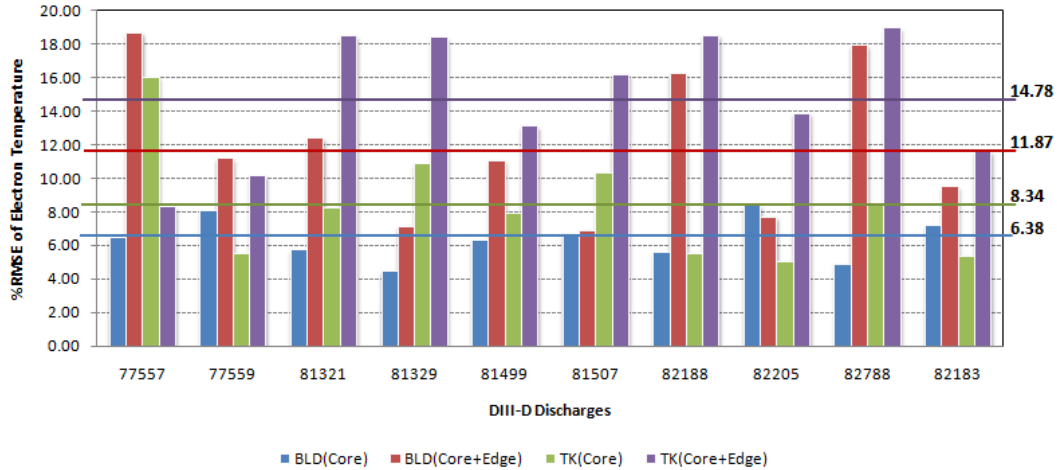


Fig. 3 The percentage of root mean square error (%RMSE) for the electron temperature profiles produced by simulation using core model (Mixed B/gB) and core-edge model from BALDUR and TASK/TR codes compared with experimental data for 10 *H*-mode discharge (pedestal occurred) listed by DIII-D device.

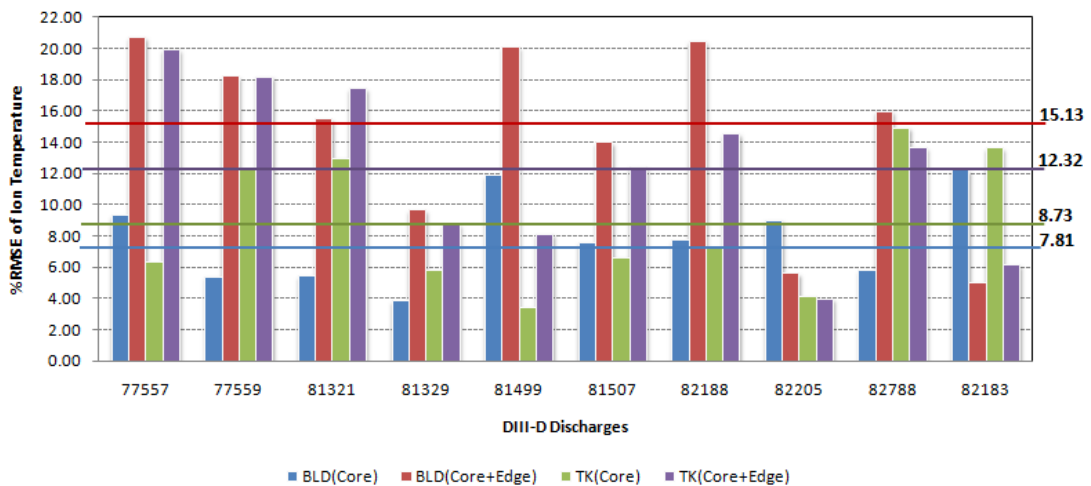


Fig. 4 The percentage of root mean square error (%RMSE) for the ion temperature profiles produced by the simulation using core model (Mixed B/gB) and core-edge model from BALDUR and TASK/TR codes compared with experimental data for 10 *H*-mode discharge (pedestal occurred) listed by DIII-D device.

In Fig.3, it shows %RMSE of the electron temperature for each discharge. The average of %RMSE of BALDUR with only core transport model equals to 6.38 and TASK/TR with core transport model equals to 8.34. After implementing the core-edge transport model to BALDUR and TASK/TR; %RMSE equals to 11.87 and 14.78, respectively. For ion temperature, %RMSE is shown in Fig.4. The average of %RMSE of BALDUR with core

transport model equals to 7.81 and TASK/TR with core transport model equals to 8.73. When the core-edge transport model has been implemented to TASK/TR and BALDUR; %RMSE equal to 12.32 and 15.13, respectively.

## 6. Conclusions

The core simulations carried out using BALDUR and TASK/TR codes with Mixed B/gB core transport model and prescribed boundary conditions yield the prediction capability with



RMSE less than 10% for both electron and ion temperature profiles. After the core-edge transport model has been implemented into both integrated predictive modeling codes, they give results whose RMSE is less than 20%. However, as mentioned above the pedestal formation will be collapsed by ELM mechanism. The complete model which includes this ELM phenomenon will be implemented to the future work to predict the dynamic edge plasma and to make the integrated predictive modeling code a more reliable tool to describe the tokamak plasmas.

### 7. Acknowledgement

This work is supported by the Commission on Higher Education (CHE) and the Thailand Research Fund (TRF) under Contract No RMU5180017 and the Commission on Higher Education, Thailand for supporting by granting fund under the program "Strategic Scholarships for Frontier Research Network for the Ph.D. Program Thai Doctoral Degree".

### 8. References

- [1] Smirnov V. P., (2010). Tokamak foundation in USSR/Russia, *Nucl. Fusion*, vol. 50, pp. 8pp.
- [2] Wagner F., Becker G., Behringer K., *et al.*, (1982). Regime of improved confinement and high beta in neutral beam heated divertor discharges of the ASDEX tokamak, *Phys. Rev. Lett.*, vol. 49(19), pp. 1408.
- [3] Singer C. E., Post D. E. and Mikkelsen D. R., (1988). A one-dimension plasma transport code, *Comput. Phys. Commun.*, vol. 49, pp. 275-398.
- [4] Honda M. and Fukuyama A., (2006). Comparison of turbulent transport models of L- and H-mode plasmas, *Nuclear Fusion*, vol. 46, pp. 580-593.
- [5] Cenacchi G. and Taroni A., (1988). JETTO: A free-boundary plasma transport code, *JET-IR*, vol. 88.
- [6] Pereverzev G. and Yushmanov P. N., (2002). ASTRA Automated System for Transport Analysis in a Tokamak, *Max-Planck Institut fur Plasmaphysik*, vol. IPP 5/98.
- [7] Basiuk V., Artaud J. F., Imbeaux F., *et al.*, (2003). Simulations of steady-state scenarios for Tore Supra using the CRONOS code, *Nuclear Fusion*, vol. 43, pp. 822.
- [8] Kinsey J. E., Staebler G. M. and Waltz R. E., (2002). Simulation of internal transport barrier formation in tokamak discharges using the GLF23 transport model, *Phys. Plasmas*, vol. 9(5), pp. 1676.
- [9] Bateman G., Kritz A. H. and Kinsey J. E., (1998). Predicting temperature and density profiles in tokamaks, *Physics of Plasmas*, vol. 5, pp. 1793.
- [10] Bateman G., Onjun T. and Kritz A. H., (2003). Integrated predictive modelling simulation of burning plasma experiment designs, *Plasma Phys. Control. Fusion*, vol. 45, pp. 1939-1960.
- [11] Kinsey J. E., Bateman G., Onjun T., *et al.*, (2003). Burning plasma projects using drift-wave transport models and scalings for the H-mode pedestal, *Nuclear Fusion*, vol. 43, pp. 1845.
- [12] Onjun T., Bateman G. and Kritz A. H., (2001). Comparison of low confinement mode transport simulation using mixed Bohm/gyro-Bohm and the Multi-Mode 95 transport model, *Phys. Plasmas*, vol. 8, pp. 975.
- [13] Hannum D., Bateman G. and Kinsey J., (2001). Comparison of high-mode



- predictive simulations using Mixed Bohm/gyro-Bohm and Multi-Mode MMM95 transport models, *Phys. Plasmas*, vol. 8, pp. 964.
- [14] Biglari H., Diamond P. H. and Terry P. W., (1990). Influence of sheared poloidal rotation on edge turbulence, *Physics of Fluids B: Plasma Physics*, vol. 2, pp. 1-4.
- [15] Gohil P., (2006). Edge transport barriers in magnetic fusion plasmas, *Comptes Rendus Physique*, vol. 7, pp. 606-621.
- [16] Boedo J., Gray D., Jachmich S., *et al.*, (2000). Enhanced particle confinement and turbulence reduction due to ExB shear in the TEXTOR tokamak, *Nucl. Fusion*, vol. 40, pp. 1397.
- [17] Oost G. V., Adamek J., Antoni V., *et al.*, (2003). Turbulent transport reduction by E x B velocity shear during edge plasma biasing: recent experimental results, *Plasma Phys. Control. Fusion*, vol. 45, pp. 1-23.
- [18] Doyle E. J., Houlberg W. A., Modelling), *et al.*, (2007). Chapter 2: Plasma confinement and transport, *Nuclear Fusion*, vol. 47, pp. S18.
- [19] Zolotukhin O. V., Igitkhanov Y., Janeschitz G., *et al.*, (2001) Transport simulations of type I ELMs, paper presented in the 28<sup>th</sup> EPS Confer. on Contr. Fusion and Plasma Phys., Funchal, Portugal.
- [20] Sugihara M., Igitkhanov Y., Janeschitz G., *et al.*, (2001) Simulation studies on H-mode pedestal behavior during type-I ELMs under various plasma conditions, paper presented in the 28<sup>th</sup> EPS Conf. on Contr. Fusion and Plasma Phys., Funchal, Portugal.
- [21] Pankin A. Y., Voitsekhovitch I., Bateman G., *et al.*, (2005). Combined model for the H-mode pedestal and ELMs, *Plasma Physics and Controlled Fusion*, pp. 483.
- [22] Janeschitz G. and *Et Al.*, (2002). A 1-D predictive model for energy and particle transport in H-mode, *Plasma Physics and Controlled Fusion*, vol. 44, pp. A459.
- [23] Pacher G. W. and *Et Al.*, (2004). Operating window of ITER from consistent core-pedestal-SOL modelling with modified MMM transport and carbon, *Plasma Physics and Controlled Fusion*, vol. 46, pp. A257.
- [24] Tala T. J. J., Heikkinen J. A. and Parail V. V., (2001). ITB formation in term of  $W_{ExB}$  flow shear and magnetic shear on JET, *Plasma Phys. Control. Fusion*, vol. 43, pp. 507.
- [25] Onjun T. and Pianroj Y., (2009). Simulations of ITER with combined effects of internal and edge transport barriers, *Nuclear Fusion*, vol. 49, pp. 075003.
- [26] Tala T., (2002) Transport Barrier and Current Profile Studies on the JET Tokamak, Doctor of Science in Technology, Helsinki University of Technology, Espoo, Finland.
- [27] Honda M., (2007) Transport simulation of tokamak plasmas including plasma rotation and radial electric field, Ph.D. Thesis, Nuclear Engineering, Kyoto University,
- [28] Boucher D., Connor J. W., Houlberg W. A., *et al.*, (2000). The International Multi-Tokamak Profile Database, *Nuclear Fusion*, vol. 40, pp. 1955.